Article

Combinatorial Discovery of Visible-Light Driven Photocatalysts Based on the ABO_3-type (A= Y, La, Nd, Sm, Eu, Gd, Dy, Yb, B = Al and In) Binary Oxides

Jianjun Ding, Jun Bao, Song Sun, Zhenlin Luo, and Chen Gao*

National Synchrotron Radiation Laboratory and Hefei National Laboratory for Physical Sciences at Microscale, University of Science and Technology of China, Hefei, Anhui 230026, China

Received February 22, 2009

A combinatorial approach was used to systematically investigate the photocatalytic activities of different kinds of ABO_3-type oxides (A = Y, La, Nd, Sm, Eu, Gd, Dy, Yb; B = Al, In). Two novel photocatalysts, cubic $YInO_3$ and perovskite $YAlO_3$, were identified rapidly. Scale-up experiments confirmed that the two photocatalysts, especially the $YInO_3$, had excellent photocatalytic activity for toluene oxidation and water splitting under visible-light irradiation.

Introduction

In the past 10 years, the development of visible-light driven photocatalysts has attracted much attention for the efficient utilization of solar energy or indoor artificial light in the splitting of water and degradation of organic pollutants. Until now, research efforts have mainly focused on the modification of TiO_2, an ultraviolet (UV) light photocatalyst, by shifting its absorption band into the visible range.[1−3] A few efforts have been carried out on the development of new materials with intrinsic visible photocatalytic activity. In this field, recent significant work of Zou, Domen and Inoue et al.[4−7] are representative of such successful examples. They have developed a series of new materials to exhibit a strong photocatalytic effect on water splitting and organic contaminant degradation under the visible-light irradiation, such as $In_{0.9}Ni_{0.1}TaO_4$ and $(Ga_{1-x}Zn_x)(N_{1-x}O_x)$.

The binary oxides with the general formula ABO_3 have various crystalline structures and show special physical chemical properties, which offer a promising matrix for the chemical substitution. Substitution in both A and B sites can change the composition and symmetry of the oxides and creates cations or oxygen vacancies, which have a major influence on the band structures, as well as the photocatalytic behavior of these materials.[8,9] For example, some oxides with ABO_3-type perovskite structure, such as $SrTiO_3$, $ATaO_3$ (A = Li, Na, K), $MCo_{1/3}Nb_{2/3}O_3$ (M = Ca, Sr, Ba), etc., have been found to show high photocatalytic activity.[10−13] These reported materials are mainly composed of alkali metal or alkaline-earth metal (A-site) and transition metal (B-site) ions. Little attention has been paid to the photocatalytic properties of rare earth ion substituted materials. On the other hand, there have been limited reports about the influence of a cation in an A-site on the properties and structures of ABO_3-type photocatalysts, since a covalent bond between B-site cation and oxygen is believed to be a main factor in determining the electronic structure as well as catalytic properties of photocatalysts.[13−15]

In the present study, we have investigated the visible light-induced photocatalytic activities of different kinds of ABO_3-type compounds (A = Y, La, Nd, Sm, Eu, Gd, Dy, Yb, B = Al and In). However, such a systematic search involves a lot of time-consuming synthesis and characterization efforts using the traditional one-at-a-time approach. To accelerate the search for advanced photocatalysts, here a combinatorial strategy, by which large collections of compounds were synthesized and screened in a materials library simultaneously for a particular physical or chemical property, was adopted. For the "lead compounds" screened out from the library, the scale-up experiments were carried out and their structures and photocatalytic properties were studied.

Experimental Section

The materials library containing ABO_3-type (A = Y, La, Nd, Sm, Eu, Gd, Dy, Yb, B = Al and In) compounds were synthesized by a parallel solution combustion synthesis technique developed in our group.[16] Compared with the solid-state reactions, solution-combustion synthesized powders are generally more homogeneous, have fewer impurities, and have higher surface area. The synthesis of library was as follows: The precursor solutions (>99.99% purity) of 1.0 $mol \cdot L^{-1}$ nitrates and 2.0 $mol \cdot L^{-1}$ glycine $C_2H_5NO_2$ were dispensed into the microwells on a ceramic substrate in a stoichiometric ratio of combustion reaction. The as-deposited

* To whom correspondence should be addressed. E-mail: cgao@ustc.edu.cn.

10.1021/cc9000295 CCC: $40.75
Published on Web 06/19/2009

library was placed in an ultrasonic tester for 30 min and then left in air for more than 24 h for diffusion. After that, the library was placed in an electrical furnace at 473 K for 30 min. The temperature was then increased to 673 K at a rate of 3 K·min^{-1}. Solution combustion (SC) reactions took place in every microwell during this period. Finally, the library was annealed at 1373 K for 12 h. Element analysis results indicated that no residual organic or carbon were found in the final products. The amount of the synthesized samples in each well was kept constant (12 mg). The yields of the SC reactions under the present conditions were about 90%.

The photocatalytic degradation of methylene blue (MB) was used as the model reaction to screen the photocatalysts library. Because the powders in the ceramic library are hard to characterize, additional steps were adopted to transfer the powders to a poly(tetra-flouro-ethylene) (PTFE) library. The microwells in the PTFE library were 10 mm in diameter and 5 mm in depth. The amount of the photocatalyst in the each well was about 12 mg. Then 0.2 mL MB solution with a concentration of 20.1 μmol·L^{-1} was dispensed into each well. The initial pH values of the solutions in the microwells were nearly 7. The library was exposed to sunlight for photocatalytic reaction. Because of the photolysis of MB itself in the visible region, the fading rate of MB cannot represent the true performance of the photocatalyst. But as all the samples in the library were measured under the same conditions, the photocatalysts library can be screened rapidly in a parallel mode by comparing the fading rates of MB solution in each well.

For the "leads" screened out from the library, the bulk samples were synthesized, and their photocatalytic activity for gaseous toluene oxidation and water splitting under visible-light irradiation was investigated. The experiments were performed using a closed gas circulation system and an outside-irradiation type reactor. The optical system used for the photocatalytic reaction consisted of a 300 W Xe arc lamp (PLS-SXE300, ChangTuo Ltd., China), a wavelength-selective beamsplitter (infrared transmission, visible/UV reflection), and an UV cutoff filter. The effective output power of the Xe arc lamp is 47 W. The light of the lamp was first reflected by the beamsplitter and then passed through the filter, before it entered the reactor cell. To eliminate any thermal effect, a water jacket was used to keep the temperature of the solution constant at room temperature by flowing cooling water. For the toluene oxidation, 0.35 g photocatalyst powder was placed at the bottom of a Petri dish inside the reactor. The reaction gas mixture consisted of 175 ppmV toluene, 22% O_2 and N_2 balance gas and 23% relative humidity. The CO_2 and toluene concentrations in the effluent gas were measured with a gas chromatograph (Kexiao GC-1690) equipped with a thermal conductivity detector (TCD), a flame ionization detector (FID) and a methane converter. The splitting of water was carried out with 0.35 g photocatalyst powder suspended in 120 mL aqueous solution containing 0.25 mol·L^{-1} Na_2S and 0.25 mol·L^{-1} Na_2SO_3 as the sacrificial agents. The H_2 evolved was analyzed on a TCD gas chromatograph (Shimadzu GC-14C, TCD sensitivity ≥5000 mVmL/mg (benzene), equipped with a carboxen 1000 column).

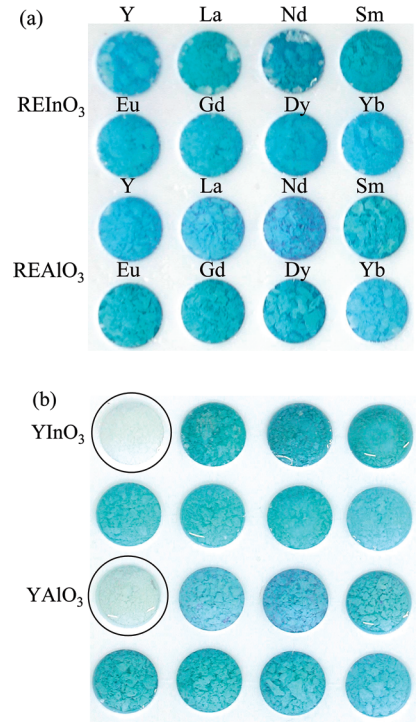

Figure 1. Photos of the library containing MB solution before (a) and after being exposed to the sunlight for about 150 min (b).

Results and Discussion

Figure 1 presents the photograph of the library before and after the photocatalytic reaction. After irradiation under sunlight for about 150 min, the color of the solutions containing $YInO_3$ and $YAlO_3$ changed from deep blue to colorless, while that of the others showed no significant change. The result indicated that the $YInO_3$ and $YAlO_3$ had a much higher photofading activity for MB solution than that of the others. The high-throughput method introduced here provides a low-cost, easy to handle, and powerful tool to screen for better photocatalysts.

X-ray diffraction (XRD) results showed that the compound of composition $YInO_3$ in the library crystallized in pure cubic structure, while the $YAlO_3$ in the library was impure and contained two other compounds $Y_3Al_5O_{12}$ and $Y_4Al_2O_9$. For further study, the scale-up experiments were performed. The bulk samples $YInO_3$, $Y_3Al_5O_{12}$, and $Y_4Al_2O_9$ were synthesized by the combustion of aqueous redox mixtures comprising stoichiometric amounts of nitrates and fuel $C_2H_5NO_2$. Taking $YInO_3$ as an example: 0.958 g $Y(NO_3)_3·6H_2O$, 0.955 g $In(NO_3)_3·9/2H_2O$ and 0.625 g $C_2H_5NO_2$ were dissolved in 20 mL deionized water. The solution was left in air more than 24 h for diffusion. After that, the mixed solution was placed in an electrical furnace at 473 K for 30 min, and then slowly heated to 673 K within 30 min. During this time, a spontaneous combustion process took place and a fluffy powder was formed. The chemical reaction in the combustion can be represented by the following equation.

$$3Y(NO_3)_3 + 3In(NO_3)_3 + 10C_2H_5NO_2 = 3YInO_3 + 25H_2O + 20CO_2 + 14N_2$$

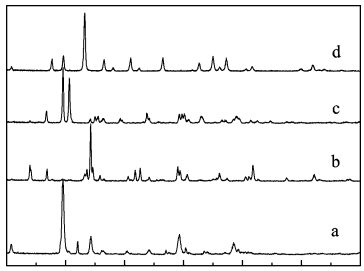

Figure 2. XRD patterns of the synthesized bulk samples: (a) $YInO_3$, (b) $YAlO_3$, (c) $Y_4Al_2O_9$, (d) $Y_3Al_5O_{12}$.

Finally, the powders were annealed at 1373 K for 12 h. The synthesis of bulk $YAlO_3$ was slightly different from the above samples. The pure phase $YAlO_3$ can be obtained by the SC method with a 25% of stoichiometric excess of nitrates.

Figure 2 presents the XRD patterns of these synthesized bulk samples. The bulk $YInO_3$ had a cubic structure, same as that of the sample in the library. The $YAlO_3$ had an orthorhombic perovskite structure, while the $Y_3Al_5O_{12}$ and $Y_4Al_2O_9$ structures were cubic and monoclinic, respectively.

Photocatalytic degradation of organic compounds is an important branch of the broader subject of photocatalysis.[17−19] Toluene is a typical volatile organic compound (VOC) and a major indoor and industrial air pollutant. Under the action of photocatalyst, toluene was first oxidized to intermediate compounds such as benzaldehyde and benzoic acid, which was further decomposed to final products CO_2 and H_2O.[20,21] A schematic of the possible degradation path of toluene is shown[21]

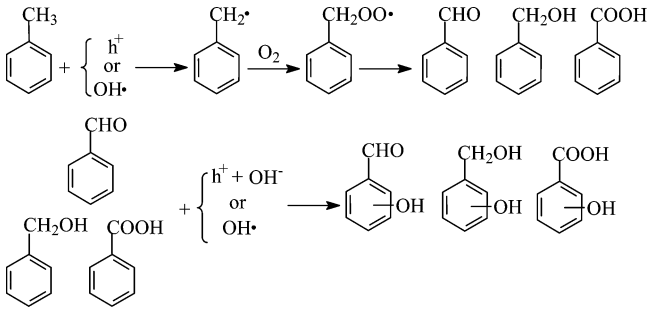

In the present study, the photocatalytic activity of the synthesized bulk samples for toluene oxidation was measured under visible-light irradiation and the results were illustrated in Figure 3. The removal ratio and mineralization ratio of toluene was calculated from the toluene and CO_2 concentrations in the effluent gas, respectively. The cubic $YInO_3$ showed excellent activity for toluene oxidation. Its toluene removal ratio and mineralization ratio were 71% and 41%, respectively. The discrepancy between the removal ratio and mineralization ratio is due to the fact that some of the reaction intermediates are stable and hardly oxidized compared with toluene.[22] The perovskite structure $YAlO_3$ exhibited considerable activity, whereas other two Y−Al−O samples: $Y_3Al_5O_{12}$ and $Y_4Al_2O_9$ showed negligible photocatalytic activity.

The water decomposition on the synthesized bulk $YInO_3$ and $YAlO_3$ under visible-light irradiation was also measured.

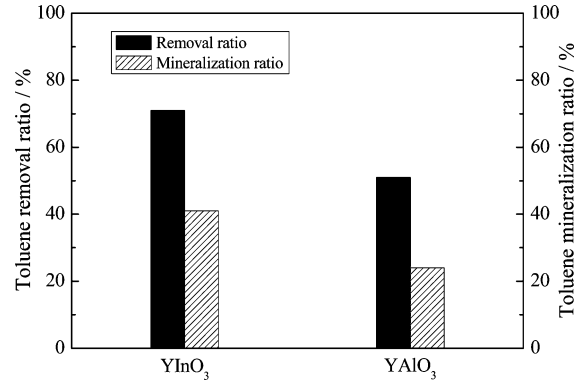

Figure 3. Removal ratio and mineralization ratio of the toluene after 360 min irradiation on the photocatalysts.

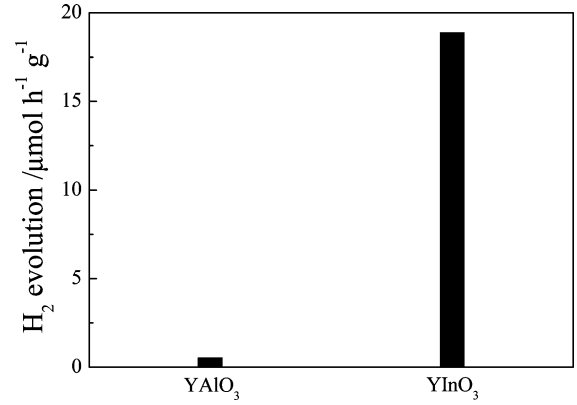

Figure 4. Photocatalytic activities of 0.5 wt % Pt-dispersed photocatalysts for water splitting under visible-light irradiation.

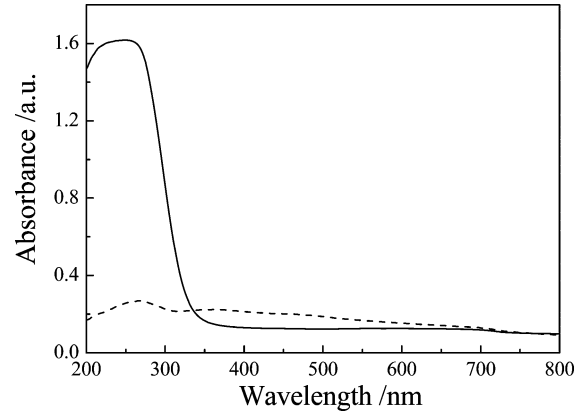

Figure 5. UV−vis diffuse reflectance spectra of the $YInO_3$ (solid line) and $YAlO_3$ (dash line).

Pt was used as a promoter to modify the photocatalysts by an incipient impregnation method using chloroplatinic acid as metal precursor. After impregnation, the samples were dried at 383 K for 24 h, and then reduced at 573 K in pure H_2 flow for 2 h. Figure 4 shows the photocatalytic activities of 0.5 wt % Pt-dispersed catalysts for water decomposition under visible-light irradiation. The $YInO_3$ exhibited excellent activity for water splitting with the dispersion of Pt. Its formation rate of H_2 evolution was 18.88 $\mu mol \cdot h^{-1} g^{-1}_{cat}$. In contrast, the activity of the Pt-dispersed $YAlO_3$ was relatively low. The stability of the $YInO_3$ and $YAlO_3$ was tested by recycling the photocatalysts two times in the toluene oxidation and water splitting, respectively. No significant loss of activity was observed. Furthermore, XRD analysis dem-

onstrated that the crystal structure of the photocatalysts did not change after reactions (not shown). The apparent quantum efficiency for H_2 evolution over the 0.5 wt % $Pt/YInO_3$ was measured using a band-pass filter ($\lambda = 420$ nm, half-width: 12 nm). The measured value was estimated to be ~0.65%. These results indicated that the screened two samples, especially the $YInO_3$, were stable and effective photocatalysts.

The UV−vis diffuse reflectance spectra of the $YInO_3$ and $YAlO_3$ are presented in Figure 5. The $YInO_3$, with significant photocatalytic activity, has weak light absorption ability in visible region. This suggested that the $YInO_3$ may have low recombination probability of photoexcited electron and hole and excellent charge transfer ability to the surface of the photocatalyst. For $YAlO_3$, no absorption edge was observed in the diffuse reflectance spectra with $\lambda > 200$ nm. Previous studies also reported that the band gap of $YAlO_3$ single crystal is about 7 eV.[23] This indicated that the $YAlO_3$ is not a typical semiconductor material. Its photocatalytic activity may be due to the fact that the material has strong absorption in visible region, as shown in Figure 5. Further studies on the geometric and electronic structures of the photocatalysts are in progress and will be reported elsewhere.

Conclusion

In a summary, the photocatalytic activities of different kinds of ABO_3-type compounds (A = Y, La, Nd, Sm, Eu, Gd, Dy, Yb, B = Al and In) were studied by a combinatorial method. Among these compounds, two novel photocatalysts: cubic $YInO_3$ and perovskite $YAlO_3$ were identified rapidly, which showed high activities for toluene oxidation and water splitting under visible-light irradiation. Furthermore, the photocatalysts had stable crystal structure and photocatalytic performance. The work gives some insight into the study of new visible-light-driven photocatalysts. The combinatorial method also provides a low-cost, easy to handle, and powerful tool for screening better photocatalysts.

Acknowledgment. This work was supported by NSFC (Grant 50721061).

References and Notes

(1) Asahi, R.; Morikawa, T.; Ohwaki, T.; Aoki, K.; Taga, Y. *Science* **2001**, *293*, 269–271.
(2) Kisch, H.; Zang, L.; Lange, C.; Maier, W. F.; Antonius, C.; Meissner, D. *Angew. Chem., Int. Ed.* **1998**, *37* (21), 3034–3036.
(3) Anpo, M.; Takeuchi, M. *J. Catal.* **2003**, *216* (1−2), 505–516.
(4) Zou, Z. G.; Ye, J. H.; Sayama, K.; Arakawa, H. *Nature* **2001**, *414*, 625–627.
(5) Tang, J. W.; Zou, Z. G.; Ye, J. H. *Angew. Chem., Int. Ed.* **2004**, *43* (34), 4463–4466.
(6) Maeda, K.; Takata, T.; Hara, M.; Saito, N.; Inoue, Y.; Kobayashi, H.; Domen, K. *J. Am. Chem. Soc.* **2005**, *127* (12), 8286–8287.
(7) Maeda, K.; Teramura, K.; Lu, D. L.; Takata, T.; Saito, N.; Inoue, Y.; Domen, K. *Nature* **2006**, *440*, 295.
(8) Song, K.; Cui, H. X.; Kim, S. D.; Kang, S. *Catal. Today* **1999**, *47* (1−4), 155–160.
(9) Poplawski, K.; Lichtenberger, J.; Keil, F. J.; Schnitzlein, K.; Amiridis, M. D. *Catal. Today* **2000**, *62* (4), 329–336.
(10) Ahuja, S.; Kutty, T. R. N. *J. Photochem. Photobiol. A* **1996**, *97* (1−2), 99–107.
(11) Konta, R.; Ishii, T.; Kato, H.; Kudo, A. *J. Phys. Chem. B* **2004**, *108* (26), 8992–8995.
(12) Kato, H.; Kudo, A. *J. Phys. Chem. B* **2001**, *105* (19), 4285–4292.
(13) Yin, J.; Zou, Z. G.; Ye, J. H. *J. Phys. Chem. B* **2003**, *107* (21), 4936–4941.
(14) Yin, J.; Zou, Z. G.; Ye, J. H. *J. Phys. Chem. B* **2003**, *107* (1), 61–65.
(15) Yin, J.; Zou, Z. G.; Ye, J. H. *J. Phys. Chem. B* **2004**, *108* (26), 8888–8893.
(16) Luo, Z. L.; Geng, B.; Bao, J.; Gao, C. *J. Comb. Chem.* **2005**, *7* (6), 942–946.
(17) Einaga, H.; Futamura, S.; Ibusuki, T. *Appl. Catal. B: Environ.* **2002**, *38* (3), 215–225.
(18) Alberici, R. M.; Jardim, W. F. *Appl. Catal. B: Environ.* **1997**, *14* (1−2), 55–68.
(19) Obee, T. N.; Brown, R. T. *Environ. Sci. Technol.* **1995**, *29* (5), 1223–1231.
(20) Cao, L. X.; Gao, Z.; Suib, S. L.; Obee, T. N.; Hay, S. O.; Freihaut, J. D. *J. Catal.* **2000**, *196* (2), 253–261.
(21) D'Hennezel, O.; Pichat, P.; Ollis, D. F. *J. Photochem. Photobiol, A* **1998**, *118* (3), 197–204.
(22) Inaba, R.; Fukahori, T.; Hamamoto, M.; Ohno, T. *J. Mol. Catal. A* **2006**, *260* (1−2), 247–254.
(23) Tomiki, T.; Kaminao, M.; Tanahara, Y.; Futemma, T.; Fujisawa, M.; Fukudome, F. *J. Phys. Soc. Jpn.* **1991**, *60* (5), 1799–1813.

CC9000295